Nuclear Instruments and Methods in Physics Research B 267 (2009) 610–614

Contents lists available at ScienceDirect

Nuclear Instruments and Methods in Physics Research B

journal homepage: www.elsevier.com/locate/nimb

Quantum interference in grazing scattering of swift He atoms from LiF(001) surfaces: Surface eikonal approximation

M.S. Gravielle *, J.E. Miraglia

Instituto de Astronomía y Física del Espacio, CONICET, Casilla de Correo 67, Sucursal 28, 1428 Buenos Aires, Argentina
Dpto. de Física, FCEN, Universidad de Buenos Aires, Buenos Aires, Argentina

ARTICLE INFO

Article history:
Received 12 September 2008
Received in revised form 27 October 2008
Available online 10 December 2008

PACS:
34.35.+a
34.50.−s
34.80.Bm

Keywords:
Channeling
Surface
Elastic scattering
Diffraction

ABSTRACT

This work deals with the interference effects recently observed in grazing collisions of few-keV atoms with insulator surfaces. The process is studied within a distorted-wave method, the surface eikonal approximation, based on the use of the eikonal wave function and involving axial channeled trajectories with different initial conditions. The theory is applied to helium atoms impinging on a LiF(001) surface along the ⟨110⟩ direction. The role played by the projectile polarization and the surface rumpling is investigated. We found that when both effects are included, the proposed eikonal approach provides angular projectile spectra in good agreement with the experimental findings.

1. Introduction

Elastic scattering of neutral atoms from insulator crystal surfaces has deserved considerable theoretical and experimental research along the years [1–4]. Lately, however, this process has attracted renewed attention as a consequence of new experiments [5–7] that show interference patterns in the distributions of atoms grazingly scattered at intermediate impact velocities, i.e. in the keV range, for which diffraction effects were not expected to be observable.

To investigate this striking phenomenon we employ a distorted-wave model – the surface eikonal approximation – which was introduced in a previous article [8]. This approach makes use of the eikonal wave function [9] to represent the elastic collision with the insulator surface, while the movement of the fast projectile is classically described, considering axial channeled trajectories with different initial conditions. The surface eikonal approximation is valid precisely for small de Broglie wavelengths of incident atoms, like those considered here, which are some orders of magnitude smaller than the shortest interatomic distance in the crystal.

Since most of the available experimental data [5–7] correspond to the He–LiF surface system, we apply the surface eikonal approximation to study angular distributions of swift He atoms elastically scattered from LiF(001) under axial surface channeling conditions. A key point in the description of the diffraction patterns is the proper representation of the projectile-surface interaction, especially in the vacuum region far from the surface plane, where grazing projectiles run. In our model, the interaction of the incident atom with the crystal surface is described as a sum of individual interatomic potentials, which take into account the contributions coming from the different ionic centres of the insulator material [10]. We evaluate the interatomic potentials within the Abrahamson approximation [11], adding the asymptotic contribution of the projectile polarization. The influence of the polarization is investigated, finding that it is important for incidence along the ⟨110⟩ channel. We also analyze the role played by the rumpling of the surface, that is, the small displacement of the surface ions with respect to their equilibrium positions as a consequence of the surface relaxation.

The work is organized as follows. The theoretical formalism is summarized in Section 2, results are presented and discussed in Section 3, and in Section 4 we outline our conclusions. Atomic units ($e^2 = \hbar = m_e = 1$) are used unless otherwise stated.

* Corresponding author. Address: Instituto de Astronomía y Física del Espacio, CONICET, Casilla de Correo 67, Sucursal 28, 1428 Buenos Aires, Argentina. Tel.: +54 11 4781 6755; fax: +54 11 4786 8114.
E-mail address: msilvia@iafe.uba.ar (M.S. Gravielle).

0168-583X/$ - see front matter © 2008 Elsevier B.V. All rights reserved.
doi:10.1016/j.nimb.2008.12.002

2. Theoretical model

Let us consider an atomic projectile (P), with initial momentum $\vec{K}_i$, which is elastically scattered from a crystal surface (S), ending in a final state with momentum $\vec{K}_f$. The frame of reference is fixed on a target ion belonging to the first atomic layer, with the surface contained in the x–y plane and the $\hat{z}$ versor perpendicular to the surface, aiming towards the vacuum region.

The T-matrix element associated with the elastic process can be defined in terms of the scattering state of the projectile, Ψ_i^+, as

$$T_{if} = \int d\vec{R}_P \; \Phi_f^*(\vec{R}_P) \; V_{SP}(\vec{R}_P) \; \Psi_i^+(\vec{R}_P), \tag{1}$$

where $\vec{R}_P$ denotes the position of the center of mass of the incident atom, V_{SP} is the surface-projectile interaction and Φ_f is the final unperturbed wave function. The state Ψ_i^+ tends to the initial unperturbed state Φ_i when the projectile is far from the surface, with $\Phi_j(\vec{R}_P) = (2\pi)^{-3/2} \exp(i\vec{K}_j \cdot \vec{R}_P)$ for $j = i(f)$.

At intermediate and high impact energies, Eq. (1) can be expressed in terms of the classical trajectory of the projectile – $\vec{\mathscr{R}}_{\mathscr{P}}$ – by means of the substitution $\vec{R}_P \cong \vec{\mathscr{R}}_{\mathscr{P}}$, like in the usual semiclassical formalism [12]. Under this assumption and taking into account that the de Broglie wavelength of the incident projectile, $\lambda = 2\pi/K_i$, is sufficiently short compared to the characteristic distance of the surface potential, it is possible to approximate the scattering state Ψ_i^+ by means of the eikonal wave function [9], i.e.

$$\Psi_i^+(\vec{\mathscr{R}}_P) \simeq \chi_i^{(eik)+}(\vec{\mathscr{R}}_P) = \Phi_i(\vec{\mathscr{R}}_P) \exp(-i\eta(\vec{\mathscr{R}}_P)), \tag{2}$$

where $\eta(\vec{\mathscr{R}}_P)$ is the eikonal phase, defined as

$$\eta(\vec{\mathscr{R}}_P(t)) = \int_{-\infty}^{t} dt' \; V_{SP}(\vec{\mathscr{R}}_P(t')), \tag{3}$$

with $\vec{\mathscr{R}}_P$ the position of the incident atom at a given time t. Classical projectile trajectories can be identified through the vector $\vec{R}_{os} = (X_o, Y_o, 0)$, sketched in Fig. 1, which determines the initial position of the projectile on the surface plane, i.e. $\vec{\mathscr{R}}_P(\vec{R}_{os}, t)$. By replacing Eq. (2) in Eq. (1), after some algebra steps the eikonal transition matrix reads [8]

$$T_{if}^{(eik)} = \int d\vec{R}_{os} \; a_{if}(\vec{R}_{os}), \tag{4}$$

where

$$a_{if}(\vec{R}_{os}) = \frac{1}{(2\pi)^3} \int_{-\infty}^{+\infty} dt \left| v_z(\vec{R}_{os}, t) \right| \times \exp[-i\vec{Q} \cdot \vec{\mathscr{R}}_P - i\eta(\vec{\mathscr{R}}_P)] \; V_{SP}(\vec{\mathscr{R}}_P) \tag{5}$$

is the transition amplitude corresponding to the classical path $\vec{\mathscr{R}}_P(\vec{R}_{os}, t)$. In Eq. (5) $v_z(\vec{R}_{os}, t)$ denotes the component of the projectile velocity perpendicular to the surface plane, $\vec{Q} = \vec{K}_f - \vec{K}_i$ is the projectile momentum transfer and the final momentum $\vec{K}_f$ satisfies the energy conservation, i.e. $K_f = K_i$.

In our frame of reference, $\vec{K}_f = K_f \; (\cos\theta_f \cos\varphi_f, \cos\theta_f \sin\varphi_f, \sin\theta_f)$, where θ_f and φ_f are the final polar and azimuthal angles, respectively and φ_f is measured with respect to the incidence direction on the surface plane (see Fig. 1). The differential probability, per unit of surface area, of elastic scattering with final momentum $\vec{K}_f$ in the direction of the solid angle $\Omega_f \equiv (\theta_f, \varphi_f)$ is obtained from Eq. (4) as $dP/d\Omega_f = (2\pi)^4 m_P^2 \, | \, \tilde{T}_{if}^{(eik)} |^2$, where $\tilde{T}_{if}^{(eik)}$ denotes the eikonal T-matrix element, normalized per unit area.

2.1. Projectile–surface interaction

A relevant magnitude within the surface eikonal approximation is the potential V_{SP}, which determines not only the eikonal phase but also the classical trajectory of the projectile. In this article the projectile-surface potential is expressed as the sum of the static and polarization contributions, i.e., $V_{SP} = V_{SP}^{(st)} + V_{SP}^{(pol)}$. The static term, $V_{SP}^{(st)}$, represents the interaction potential between the atom and the crystal surface derived by assuming that their electronic densities remain invariable when the atom approaches the surface, while $V_{SP}^{(pol)}$ takes into account the rearrangement of the projectile charge as a consequence of the presence of the ionic surface. Notice that in V_{SP} we have not included the dynamic response of the surface [10] because this contribution is expected to play a minor role for neutral projectiles.

Due to the insulator character of the LiF material, formed by alkali and halide ions with closed shell structures, the surface

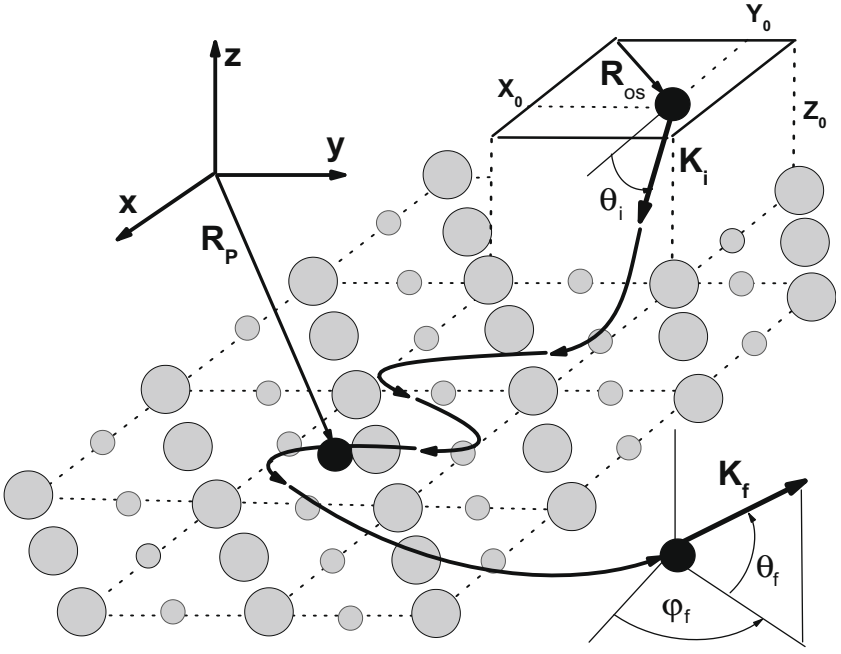

Fig. 1. Schematic depiction of the coordinate system.

can be considered as composed of independent target ions, which keep their electronic structures as they were isolate. Then, the static potential $V_{SP}^{(st)}$ can be derived by adding the individual interatomic potentials, $V_{st}(\vec{R})$, which represent the static interaction of the incident atom with solid ions placed at different lattice sites [10]. We evaluated $V_{st}(\vec{R})$ within the Abrahamson model [11], which includes the electrostatic Coulomb interaction plus the kinetic and the exchange contributions, as given in [8]. The potential $V_{SP}^{(pol)}$ is produced by the polarization of the neutral atom induced by the presence of target ions. Its asymptotic expression reads

$$V_{SP}^{(pol)}(\vec{R}) = -\frac{\alpha}{2}\left|\sum_i \frac{Z_{Ti}^{(\infty)}}{(R_{0i}^2 + R_i^2)}\hat{R}_i\right|^2, \quad (6)$$

where the sum formally includes all the target ions of the crystal and α is the polarizability of the incident atom, with α = 1.38 a.u. the static value for Helium [13]. Note that at the impact energy here considered, dynamical effects of the polarization are expected to play a minor role. In Eq. (6), $\vec{R}_i$ represents the position vector of the projectile with respect to the target ion labelled as i, with $\hat{R}_i = \vec{R}_i/R_i$, and $Z_{Ti}^{(\infty)}$ is the asymptotic charge of the target ion, being $Z_{Ti}^{(\infty)} = 1$ for Li^+ and $Z_{Ti}^{(\infty)} = -1$ for F^-. At short distances, the polarization contribution coming from the target ion i is reduced with the cutoff $R_{0i} = \langle r\rangle_{Ti} + \langle r\rangle_P$, where $\langle r\rangle_{Ti}$ and $\langle r\rangle_P$ are the target and projectile mean radii, respectively.

3. Results

The proposed model is applied to He^0 atoms elastically scattered from a LiF crystal surface, under axial surface channeling conditions. In accord with [14], F^- (Li^+) surface ions of the topmost atomic layer were displaced a distance d = 0.037 a.u. above (below) the ideal (unreconstructed) surface plane. To evaluate He–Li^+ and He–F^- static interatomic potentials within the Abrahamson model, we employed electronic densities derived from Hartree–Fock Slater wave functions [15]. At every point, the potential V_{SP} was calculated by including the contributions of the 4th order nearest neighbor target ions, which involves four atomic layers of the solid. Details of the calculation of the potential are given in [8].

Classical projectile trajectories were derived from Newton equations associated with the potential V_{SP} by using the Runge-Kutta method. Under axial surface channeling conditions, all trajectories verify the relation $\theta_f^2 + \varphi_f^2 \approx \theta_i^2$, with θ_i the glancing incidence angle, in agreement with the experimental data [5–7]. The integration on $\vec{R}_{os}$ involved in Eq. (4) was evaluated with the MonteCarlo technique. To obtain de differential probability $dP/d\Omega_f$ we added the contributions coming from different values of $\vec{R}_{os}$ that lead to the same final angle Ω_f by employing a grid for θ_f and φ_f of 100 × 100 points. In all the cases around 2×10^5 classical trajectories with random initial positions were considered.

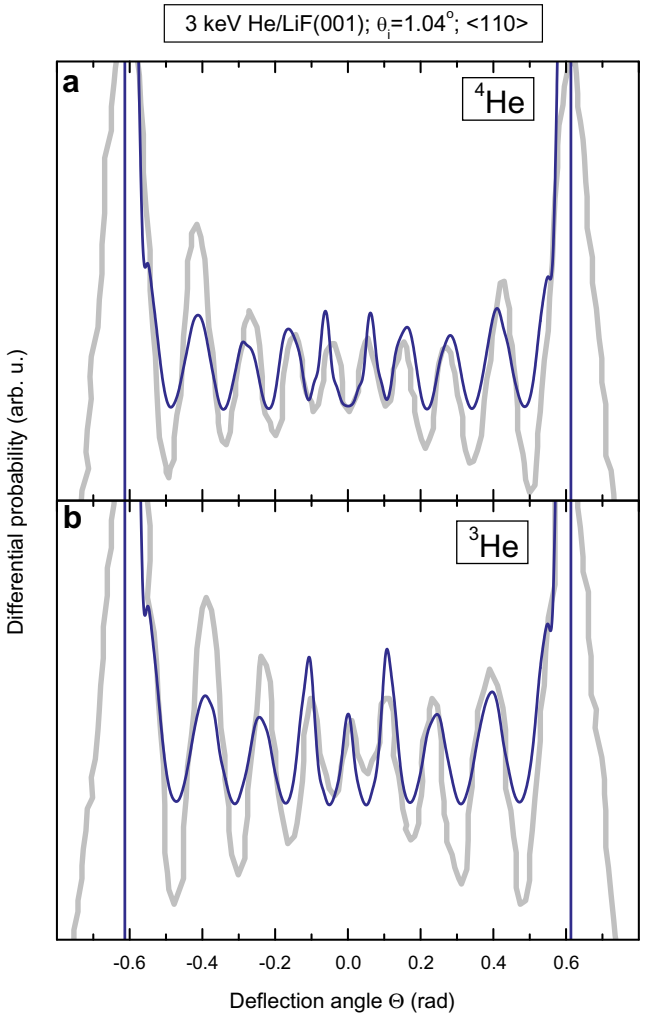

Fig. 2. Angular distribution of elastic scattered projectiles, as a function of the deflection angle Θ, for helium atoms colliding with LiF(001) along the direction ⟨110⟩. The impact energy is 3 keV and the incidence angle is 1.04°. Projectiles (a) ^{4}He and (b) ^{3}He are considered. Solid line, differential probability derived from the surface eikonal approach; thick solid line, experimental intensity drawn from Fig. 3 of [7].

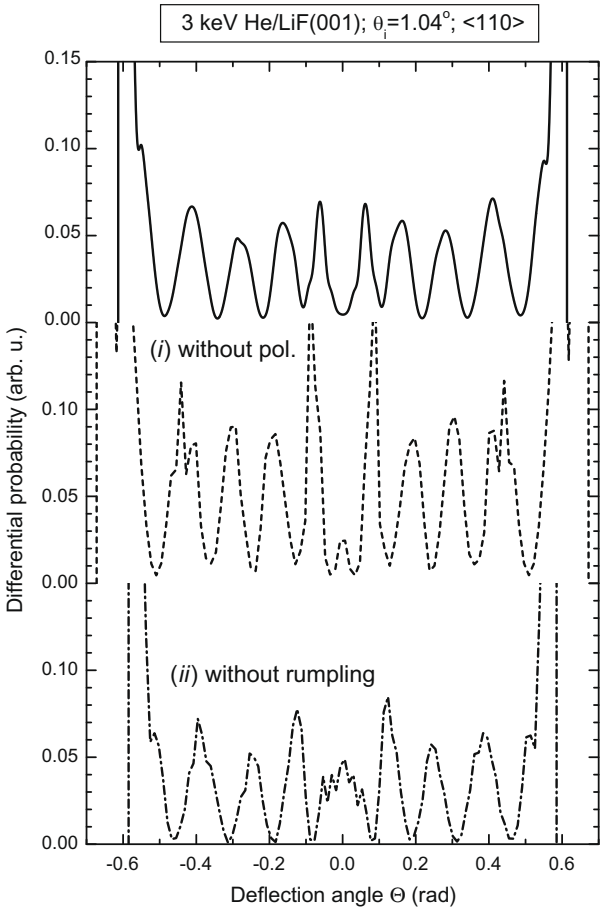

Fig. 3. Similar to Fig. 2(a). Solid line, eikonal distribution, including polarization and rumpling (d = 0.037 a.u.); dashed and dash-dotted lines, eikonal results without including (i) polarization and (ii) rumpling, respectively.

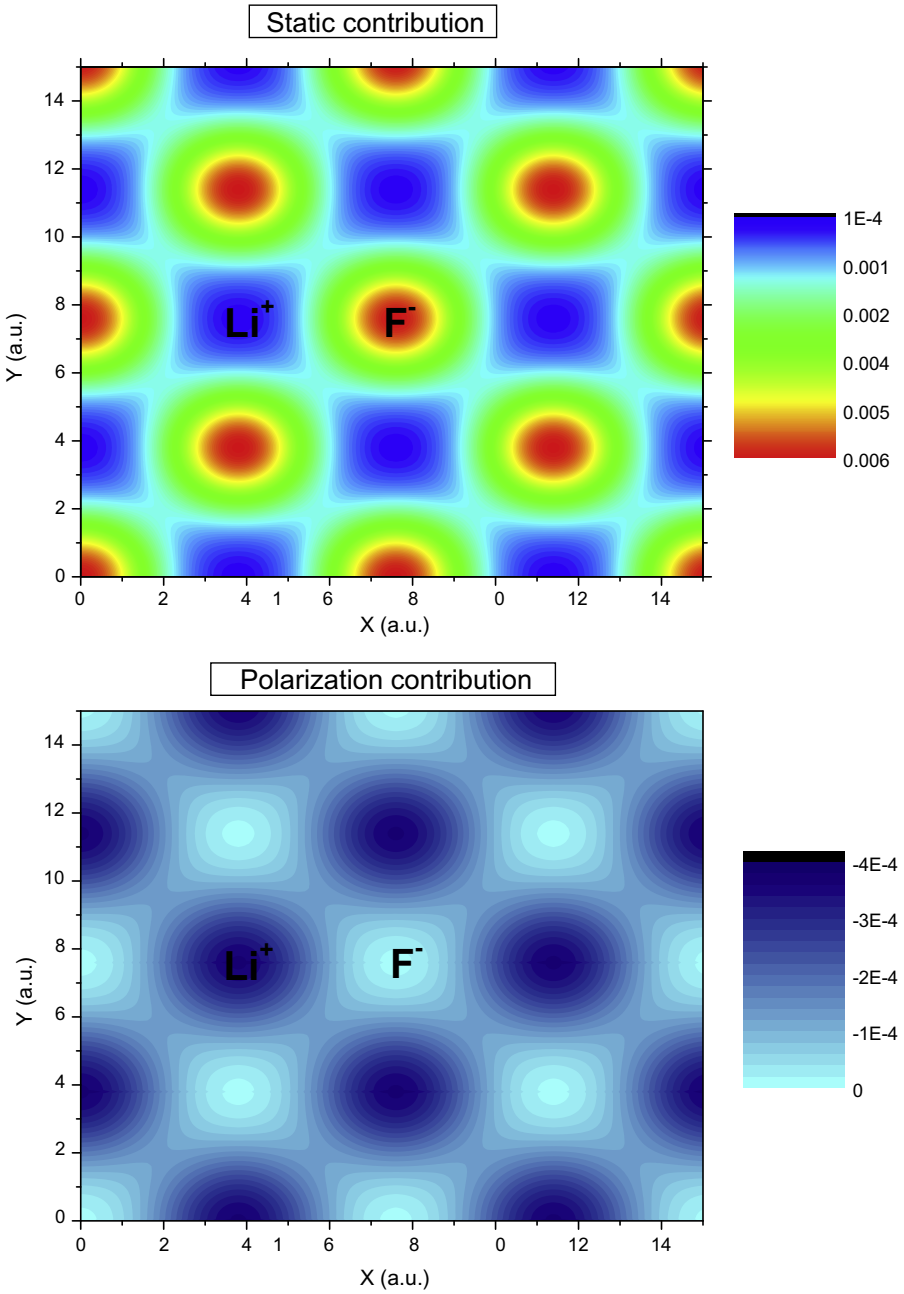

Fig. 4. Partial contributions to the projectile-surface potential, as a function of the coordinates on the surface plane, for the system He–LiF(0 0 1) at a distance $Z = 4$ a.u. from the surface (a) static and (b) polarization contributions.

In Fig. 2 we plot distributions of neutral helium atoms after colliding with a LiF(0 0 1) surface along the direction $\langle 1\,1\,0\rangle$. Like in the experiments of [7], two different isotopes of helium – ^{4}He and ^{3}He – impinging with the same energy (3 keV) and angle ($\theta_i = 1.04$deg) are considered. From Fig. 2(a) and (b), we observe that the eikonal differential probability $dP/d\Theta$ displays an oscillatory pattern as a function of the deflection angle Θ, defined as $\Theta = \arctan(\varphi_f/\theta_f)$. In both figures eikonal spectra are in close agreement with the experimental ones, reproducing almost exactly the positions of maxima, which are symmetrically placed with respect to the incidence direction, i.e. $\Theta = 0$. However, the relative intensities of the peaks are not completely well reproduced by the theory. At this point we should mention that our theoretical results were obtained without including the thermal vibration of the lattice and they were not convoluted with the experimental conditions. Both effects may produce a broadening of the angular distribution, modifying the intensities of eikonal maxima.

On the other hand, differences between the spectra of Fig. 2(a) and (b) can be adjudicated only to the different atomic masses. Eikonal distributions of the two isotopes present identical extreme angles. But the central zone of the spectrum is clearly affected by the projectile mass, showing a minimum of probability at $\Theta = 0$ for ^{4}He while for ^{3}He the central angle corresponds to a maximum. The sharp peaks placed at the extreme angles of the spectrum are associated with rainbow scattering, being also present in the classical distribution [8]. Consequently, since classical trajectories are independent of the projectile mass, these maxima are not affected by the mass variation. In turn, the oscillatory structures between the two rainbow angles are a consequence of the quantum interference between projectiles ending in the same final state but with

different transition amplitudes. From Eq. (5), a_{if} depends on the projectile mass through the classical velocity $\vec{v}$, which is not only involved in the momentum transfer $\vec{Q}$ but also in the time integration of the eikonal phase. Hence, eikonal interference structures vary with the projectile mass, showing different patterns for ^{4}He and ^{3}He atoms.

As eikonal spectra were found to be extremely sensitive to the surface-projectile potential, we analyze the role played by the projectile polarization and the surface rumpling in the eikonal distribution. In Fig. 3 we show the eikonal profile of Fig. 2(a) together with differential probabilities derived within the eikonal model but without including contributions coming from: (*i*) the polarization and (*ii*) the rumpling. We found that both effects – polarization and rumpling – strongly modify the interference structures in the central zone of the spectrum, while the external maxima, associated with classical rainbow scattering, remain almost unchanged. When $V_{SP}^{(pol)}$ is not taken into account, the shape of the distribution around $\Theta = 0$ is altered: the positions of interference maxima are shifted to highest values and a small central peak arises. Something similar happens when the rumpling is neglected in the eikonal model, that is, when an unreconstructed surface, with Li^+ and F^- surface ions placed in the same topmost plane, is considered. In this case the eikonal distribution displays a broad central maximum, the number of peaks of the eikonal spectrum being reduced to 9, in disagreement with the experimental findings. We have observed that polarization and rumpling effects on eikonal spectra vary with the incidence conditions and, in some way, they might play similar roles. In particular, for impact along the crystallographic direction $\langle 1\,0\,0\rangle$ the influence of the polarization was found to be negligible [8]. This fact is a consequence of the crystal ordering that originates an effective polarization potential along the $\langle 1\,1\,0\rangle$ direction, formed by alternate cation and anion rows. While in the $\langle 1\,0\,0\rangle$ channel, rows present a neutral charge, which reduces the polarization of the incident atom.

Under the impact conditions of Fig. 2, helium atoms that reach the central zone of the spectrum move just over Li^+ and F^- rows, presenting turning points at a distance farther than 2 a.u. from the surface. For a better understanding of the influence of the polarization, in Fig. 4 we show the static $V_{SP}^{(st)}$ and polarization $V_{SP}^{(pol)}$ contributions at a distance $Z = 4$ a.u., which corresponds to the characteristic region of the projectile movement just before entering in the close collision zone. At this distance the static potential presents a symmetrical corrugated structure, with maxima and minima placed on F^- and Li^+ sites, respectively. Also the potential $V_{SP}^{(pol)}$ displays a similar corrugated shape but with negative values, reinforcing the attractive behavior of the static potential over cation places, while over anion positions the polarization only slightly reduces the repulsion produced by $V_{SP}^{(st)}$. Therefore, the polarization increases the amplitude of the surface corrugation, modifying the relative phases of the eikonal transition amplitudes corresponding to projectiles that end around $\Theta = 0$.

4. Summary

Motivated by recent experimental works [5–7], we have employed the surface eikonal approach to study the elastic scattering of neutral atoms from insulator crystal surfaces in the intermediate energy range. In this article, the model was applied to 3 keV He atoms grazing impinging on a LiF(0 0 1) surface along the crystallographic direction $\langle 1\,1\,0\rangle$. Eikonal spectra of scattered projectiles present clear signatures of quantum interference, caused by the coherent addition of transition amplitudes corresponding to atoms that follow different paths but end up scattered with the same final momentum. As the projectile distribution strongly depends on the projectile-surface interaction, we have analyzed the influence of the projectile polarization and the surface rumpling on the angular spectrum. We conclude that for the considered collision system both effects are essential to describe the elastic scattering in the forward direction. Even though the employed rumpling is very small, it can produce substantial changes in the central zone of the eikonal distribution. Angular spectra derived from the proposed eikonal model, including polarization and rumpling contributions, are in good agreement with the available experimental data [7]. However, a detailed description of the surface potential, taking into account that target ions are part of a surface, might modify the present results.

Acknowledgements

This work was supported by CONICET, UBA and ANPCyT of Argentina.

References

[1] N. Cabrera, V. Celli, F.O. Goodman, R. Manson, Surf. Sci. 19 (1970) 67.
[2] G. Boato et al., J. Phys. C 6 (1973) L394.
[3] L.M. Hubbard, W.H. Miller, J. Chem. Phys. 78 (1983) 1801.
[4] V. Celli, D. Eichenauer, A. Kaufhold, J.P. Toennies, J. Chem. Phys. 83 (1985) 2504.
[5] A. Schüller, S. Wethekam, H. Winter, Phys. Rev. Lett. 98 (2007) 016103.
[6] P. Rousseau, H. Khemliche, A.G. Borisov, P. Roncin, Phys. Rev. Lett. 98 (2007) 016104.
[7] A. Schüller, H. Winter, Phys. Rev. Lett. 100 (2008) 097602.
[8] M.S. Gravielle, J.E. Miraglia, Phys. Rev. A 78 (2008) 022901.
[9] C.J. Joachain, Quantum Collision Theory, North-Holland, Amsterdam, 1979.
[10] A.J. García, J.E. Miraglia, Phys. Rev. A 74 (2006) 012902.
[11] A.A. Abrahamson, Phys. Rev. 133 (1964) A990.
[12] M.R.C. McDowell, J.P. Coleman, Introduction to the Theory of Ion–Atom Collisions, North-Holland, Amsterdam, 1970.
[13] T.M. Miller, B. Bederson, in: D.R. Bates, B. Bederson (Eds.), Advances in Atomic and Molecular Physics, Vol. 13, Academic, New York, 1977, p. 1.
[14] J. Vogt, H. Weiss, Surf. Sci. 501 (2002) 203.
[15] E. Clementi, C. Roetti, At. Data Nucl. Data Tables 14 (1974) 177.